Proceedings SPIE "**Novel In-Plane Semiconductor Lasers IV** " vol. 5738, p. 416-424, April 2005

High-power ridge-waveguide and broad-area lasers with a DFB resonator in the wavelength range 760-790nm

A. Klehr*, M. Braun F. Bugge, G. Erbert, J. Fricke, A. Knauer, P. Ressel, H. Wenzel and G. Tränkle

Ferdinand-Braun-Institut für Höchstfrequenztechnik, Gustav-Kirchhoff-Straße 4, 12489 Berlin, Germany

ABSTRACT

Experimental investigations on RW and BA DFB lasers emitting in the wavelength range between 760 and 790 nm are presented. The maximum output powers are 300 mW and 2.4 W for the RW and BA devices, respectively. The optical spectra of the RW DFB lasers show single mode emission with a side-mode suppression ratio of about 50 dB. The profile of the lateral far field reveals stable lasing of the fundamental lateral mode without any beam steering up to 250 mW power. The spectral linewidth of the RW devices is < 2 MHz and sufficiently small for spectroscopic applications (e.g. D_2 line of rubidium vapor). The BA devices have a full $1/e^2$ width of the spectrum of 0.08 nm at 0.5 W and 0.16 nm at 2 W.

Keywords: Semiconductor lasers, distributed-feedback lasers, ridge-waveguide lasers, broad-area leasers, high-power lasers

1. INTRODUCTION

Diode lasers emitting in the wavelength range between 760 and 790 nm are of particular interest for applications in absorption spectroscopy (e.g. oxygen, rubidium), state selection in rubidium atomic clocks, Doppler laser cooling of rubidium atoms, Raman spectroscopy and nonlinear frequency conversion which need besides a stable lasing frequency a high output power. It can be realized with a common Fabry-Perot (FP) diode laser placed together with a grating into an external cavity configuration, which necessitates, however, expensive mechanical and thermal stabilization measures /1/. Another possibility is the integration of a Bragg grating directly into the internal laser cavity. In distributed Bragg reflector (DBR) lasers the Bragg grating is located in a part of the laser cavity only and is operated passively, i.e. without current injection. In contrast, in distributed feedback (DFB) lasers the grating is integrated in the epitaxial layer structure over the whole cavity and is hence operated actively.

Whereas applications like Raman- and absorption spectroscopy or atomic clocks require single lateral mode operation and a very small spectral linewidth, other applications as IR-spectroscopy in liquids and interferometric measurements do not have so stringent demands on the lateral optical field and spectrum. In the first case, ridge-waveguide (RW) lasers operating in a single lateral mode with an output power in the range of several hundreds of milliwatts are the best option. In the second case, multi-mode broad-area (BA) lasers can be used with a 10 times higher optical output power. Note, that multiple-lateral mode operation leads inevitably to a broadening of the spectral line.

The fabrication of lasers with an integrated Bragg grating requires additional technological efforts compared to Fabry-Perot lasers. DFB and DBR laser structures can be fabricated either in single or in multiple growth steps. Single-growth DFB and DBR lasers use laterally coupled or deeply etched gratings, respectively /2,3/. So far, operation of single-stripe devices at high output power was not demonstrated yet. Additionally, laterally coupled RW DFB lasers favor the first order lateral mode and hence might exhibit mode instabilities or beam steering at high output power. Moreover, the lateral-coupling scheme cannot be used in BA lasers at all. In contrast, DBR and DFB lasers fabricated with a two-step epitaxy can reach a high output power of more than 100 mW /4,5/.

The disadvantage of DBR lasers is a periodic non-linearity in the light-current characteristics due to longitudinal mode hopping /6/. DFB lasers can operate in the same longitudinal mode over a large current range and the emission wavelength can be easily continuously tuned by changing the heatsink temperature or the operational current. Hence, DFB lasers are better suited for most applications. In the late 1980s and early 1990s, DFB lasers emitting between

* E-mail: klehr@fbh-berlin.de

760 nm and 790 nm were developed in several laboratories, cf. /7,8/ and the references therein. The highest output power reported was 10 mW in /7/ and 25 mW in /8/.

In /5/ we presented a RW DFB laser emitting 200 mW in a single lateral and longitudinal mode at a wavelength of 783 nm. In this paper, we give further experimental details such as the spatial and spectral characteristics and we present additional results at adjacent wavelengths. Furthermore, characteristics of BA DFB lasers are provided.

2. LASER STRUCTURE AND FABRICATION PROCEDURE

The DFB lasers were grown by low-pressure metal organic vapor phase epitaxy (MOVPE) in two steps, similarly as described in /9/. The layer sequence is schematically drawn in Figure 1. The first growth step consisted of a n-GaAs buffer, n-AlGaAs cladding, 250 nm n-AlGaAs waveguide, 14 nm tensile-strained GaAsP active quantum well (QW), 250 nm p-AlGaAs waveguide, the first part of the p-AlGaAs cladding and an InGaP/GaAsP/InGaP layer sequence in which the second-order grating was formed by holographic photolithography and wet-chemical etching. After surface cleaning, in the second step the remainder of the p-AlGaAs cladding and a p-GaAs contact layer were grown.

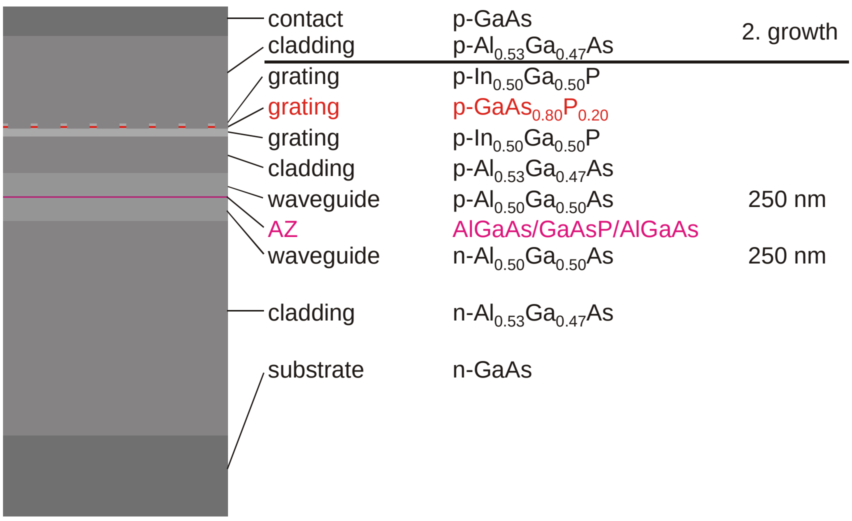

Figure 1. Transverse cross section showing epitaxial layer sequence of the 7xx-nm DFB lasers investigated.

The grating period of the fabricated 7xx-nm DFB lasers is about 220-240 nm (see Fig. 2). The exact value must be chosen in correspondence to the intended lasing wavelength. The coupling coefficient κ of the Bragg grating depends mainly on the thickness and the composition of the GaAsP grating layer and its distance to the active zone. This allows a simple adjustment of κ.

Lateral optical confinement and p-contacting is provided by a 2-3 µm wide ridge-waveguide formed by reactive ion etching and deposition of SiN_x which is opened at the top of the RW before the p-metallization is performed (see Fig.3). The BA lasers have a ridge width of 50 µm.

After substrate thinning and n-metallization, the wafers were cleaved into bars with a cavity length of 1.5 mm. The facets were anti- and high-reflection coated, which resulted in reflection coefficients of 10^{-4} and 0.95, respectively. Finally, the RW devices were soldered p-side up on AlN submounts and attached to copper heatsinks, whereas the BA lasers were soldered p-side down on C-mounts using CuW submounts.

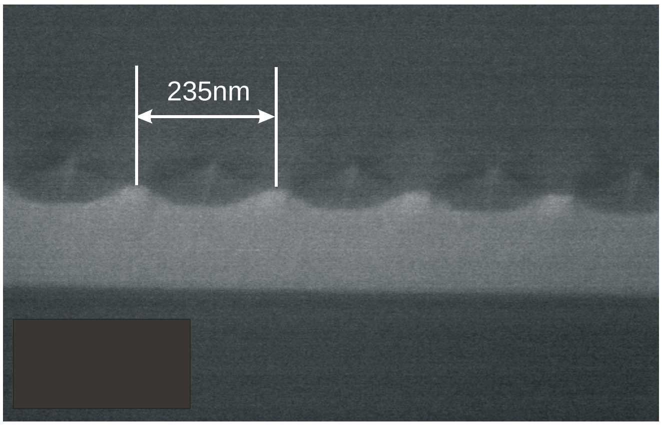

Figure 2. SEM picture showing the buried second order Bragg grating.

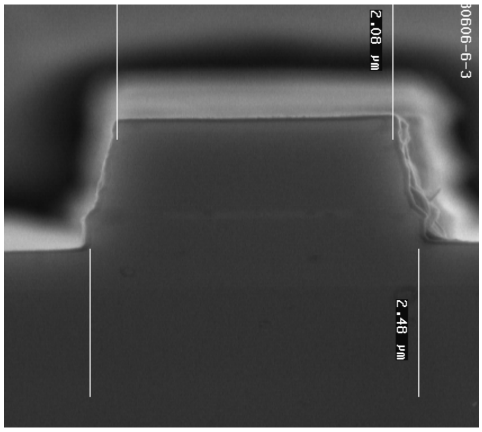

Figure 3. SEM picture of the epitaxial layer structure showing the ridge waveguide.

3. EXPERIMENTAL RESULTS

3. 1. RW DFB lasers

Fig. 4a shows the light-current (L-I) characteristics of a 780-nm DFB laser measured in CW operation. Due to the tensile-strained QW the laser emission is TM polarized. The optical power was detected with an integrating sphere. The threshold current is 48 mA and the slope efficiency is 0.76 W/A up to an output power of 200 mW. A further increase of the operating current leads to a decrease of the efficiency due to the self-heating of the laser. A maximum output power of more than 300 mW is achieved. The insets show the vertical and lateral far field profiles at an injection current of 460 mA corresponding to 250 mW power. The nearly Gaussian shape of the lateral farfield profile with a full width at half maximum (FWHM) of 12.1 degrees indicates fundamental lateral mode operation. The FWHM of the vertical farfield profile is 20.9 degrees.

In Fig. 4b the CW L-I characteristics of RW DFB lasers emitting at different wavelengths λ are compared. The threshold current of the 783-nm device is 29 mA, the other lasers have a threshold current of 42 mA. The slope efficiency of the 783- and 773-nm devices is 0.91 W/A slightly above threshold. The 763-nm device has a slope efficiency of 0.62 W/A. The differences in the electro-optical parameters are mainly caused by different RW etch depths, coupling coefficients of the Bragg grating and peak gain wavelengths of the QWs. The high efficiency is the result of the small coupling coefficient κ of the Bragg grating and low optical losses. From a fit of the emission spectrum measured below threshold to a theoretical model /10/, a real part of κ of about 1.0 cm^{-1} was determined resulting in a κL value of 0.15 (laser length 1500µm). The dips in the L-I characteristics of the 763-nm devices are caused by absorption lines of oxygen /11/.

Optical spectra were measured with an optical spectrum analyzer Q8384 with a resolution of 10 pm. A mapping of the optical spectrum of the 780 nm DFB laser (see Fig. 4a) versus current is shown in Fig. 5. Stable single-longitudinal mode operation can be observed up to more than 250 mW. A mode hop from one side of the stop band to the other occurs between at 235mA. The non-linear increase of the lasing wavelength, as can be seen in Fig. 5a, is mainly caused by a temperature induced change of the refractive indices due to Joule heating. From the wavelength shift of 1.5 nm between 100 mA and 500 mA a temperature rise of $\Delta T = 27°C$ of the active zone can be deduced on the basis of a temperature coefficient of $\Delta\lambda/\Delta T = 0.055$ nm/K determined near threshold.

The optical spectra of the DFB lasers emitting at 783 nm, 773 nm and 763 nm (see Fig. 4b) are depicted in Fig. 6. The spectra measured at 200 mW (783 nm), 150 mW (773 nm) and 100 mW (763 nm) reveal single-longitudinal mode lasing with a side-mode suppression ratio of about 50 dB. The spectral width is limited by the resolution of the optical spectrum analyzer used.

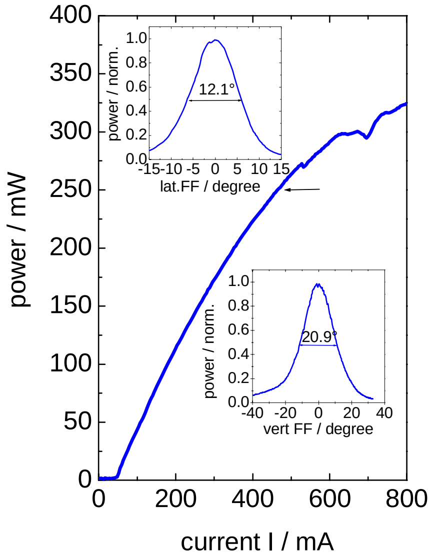

Figure 4a. CW light-current characteristics of a 780 nm RW DFB laser at 25°C. Insets: Normalized lateral (top) and vertical (bottom) farfield profiles at an output power of 250 mW (see arrow).

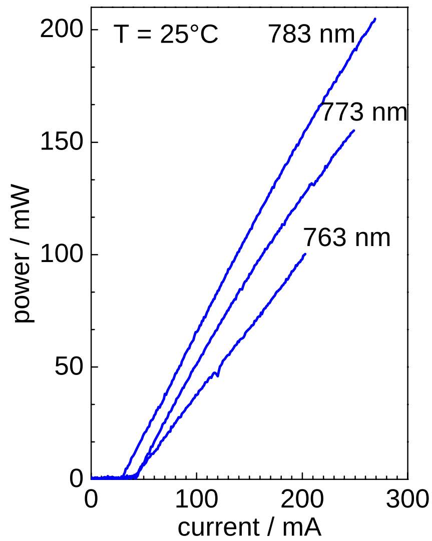

Figure 4b. CW light-current characteristics of RW DFB lasers emitting at 763, 773 and 783 nm at a temperature of 25°C.

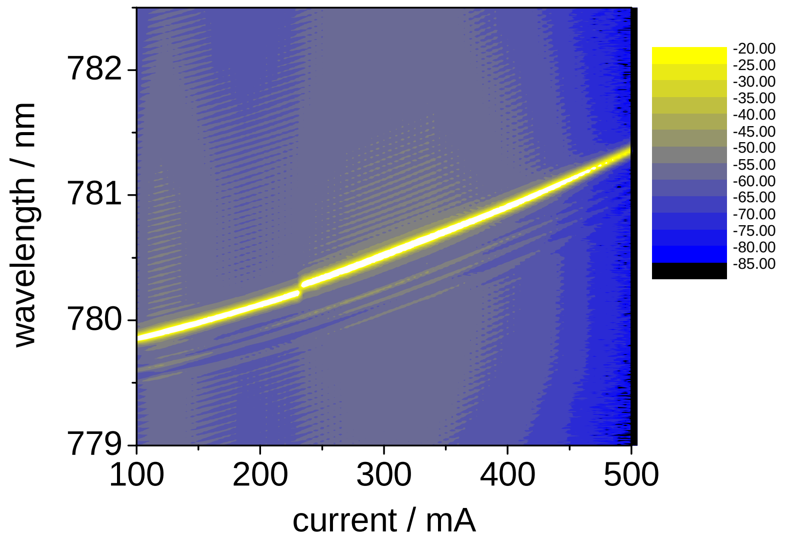

Figure 5. Mapping of the optical spectrum of the laser of Fig. 4a recorded with OSA Advantest Q8384 in the current range 100-500 mA.

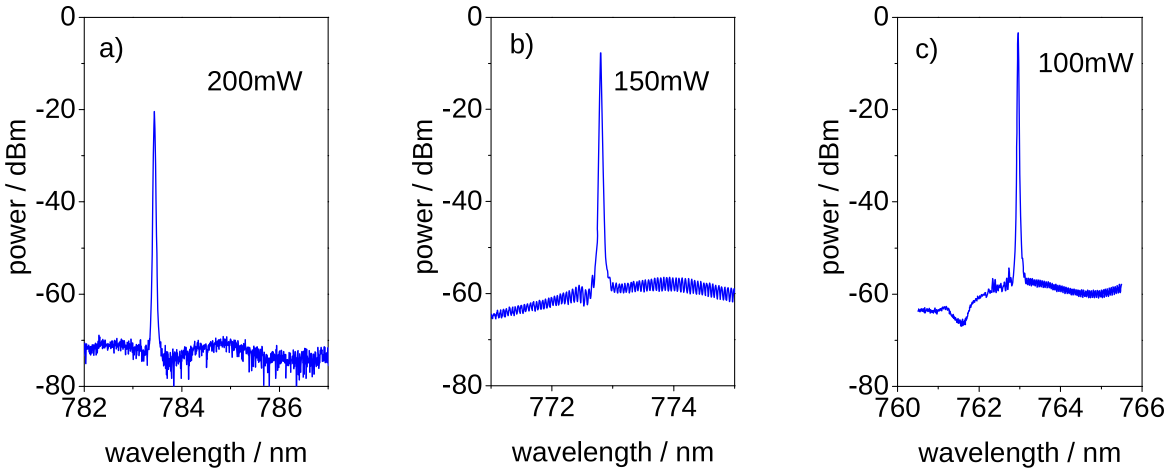

Figure 6. Optical spectra of the same devices as in Fig.4b measured at 200 mW for the 783 nm DFB laser (a), for 773 nm at 150 mW (b) and for 763 nm at 100 mW (c).

In order to determine the spectral linewidth of the lasing mode of a 780-nm DFB laser (see Fig. 4), the fluctuations of the laser radiation were measured using a homodyne fiber Mach-Zehnder interferometer with phase quadrature /12/. The laser was driven using a stabilized electrical power supply with current control. The heat sink temperature was held constant to better than 2 mK. The optical spectrum at an output power of 200 mW measured with 10 ms averaging time is shown in Fig. 7. The FWHM of the Lorentzian fit is 2 MHz, the resolution of our experimental setup.

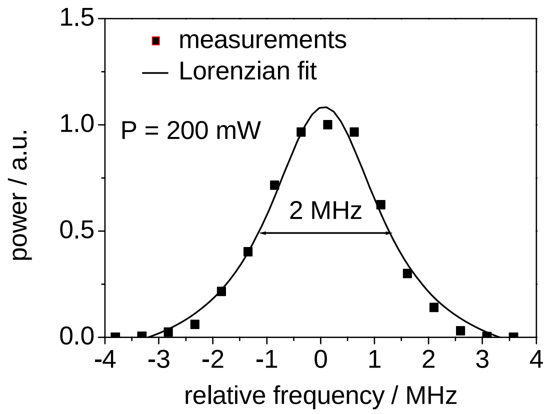

Figure 7. Spectral shape of the laser mode of a 780 nm DFB laser at an output power of 200 mW.

Tunable high-power lasers with a small spectral linewidth are very attractive for atomic clocks and spectroscopy investigations. DFB lasers emitting at a wavelength of about 780 nm can be used for spectroscopic investigations of the rubidium D_2 line (780.08 nm). In order to verify this, the output beam from the 780-nm DFB laser was collimated and passed through a rubidium cell and detected with a photodiode. In the experiments a glass cell filled with rubidium vapor having a path length of 80 mm was used. The wavelength of the lasing emission is tuned by increasing the laser current as can be seen in Fig. 8a. Here the current is increased from 160 to 190 mA and the measured wavelength shift is $\Delta\lambda/\Delta I = 0.004$ nm/mA. The small nonlinearities are due to the limited resolution of the OSA. In Fig. 8b the L-I characteristics measured behind the rubidium vapor cell is shown. With increasing current the output power increased. At 175 mA the wavelength of the DFB laser coincides with the D_2 line of the rubidium and two absorption peaks can be observed. This experiment shows, that the spectral linewidth of the solitary laser is already sufficiently small for spectroscopic applications.

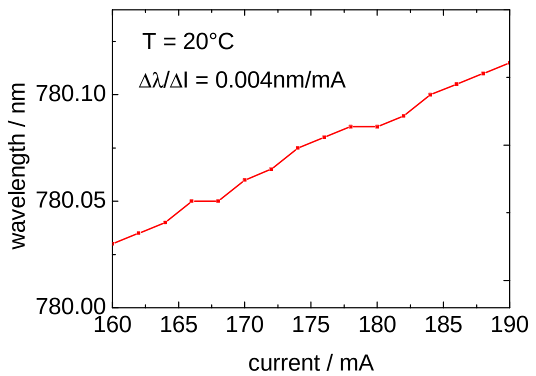

Figure 8a. Wavelength tuning behavior by variation of the injection current.

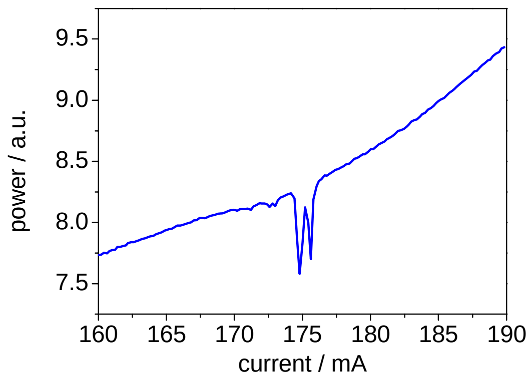

Figure 8b. CW light-current characteristic of a 780-nm DFB laser measured after the passage of the emitted radiation through a rubidium vapor cell.

In Fig. 9 results of an aging test at a power level of 150 mW at T = 25°C are shown for five 773 nm DFB lasers. The test had an overall duration of 2000 h. None of the five lasers tested failed during this time. The degradation rates were below 1.3 x 10^{-5} h^{-1} for all devices. From this rate a lifetime larger than 15000 h can be extrapolated (20 % current increase).

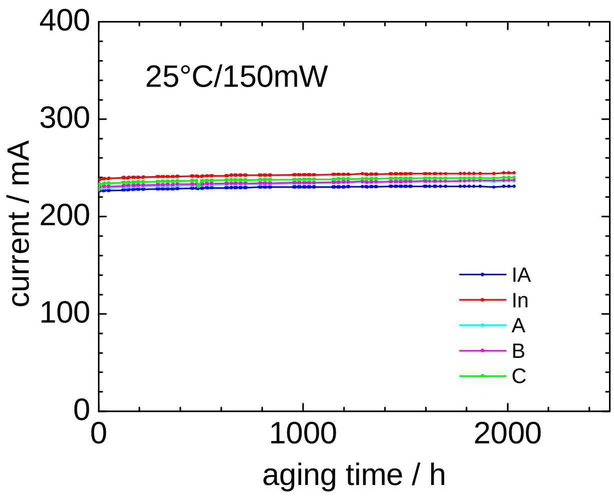

Figure 9. Aging behavior of five 1.5 mm long 773-nm DFB lasers at T = 25°C and an output power of 150 mW.

3. 2. BA DFB lasers

Whereas the reliable output power of the investigated RW DFB lasers is limited to values below 200 mW, BA DFB lasers with a stripe width of 50 µm are capable of emitting 1 W and more on the expense of multiple-lateral mode operation and hence a broader spectral line. Fig. 10 shows the CW light-current characteristic of a BA DFB laser made from the same wafer as the 783-nm RW DFB device. The threshold current is 210 mA and the slope efficiency is as high as 0.98 W/A up to an output power of 1.5 W. A further increase of the power leads to a decrease of the efficiency due to self heating. At an injection current of 3 A a maximum output power of 2.4 W is achieved. The insets show the lateral and vertical far field profiles at an output power of 1.5 W. The lateral farfield profile has a FWHM of 9.3 degrees. The FWHM of the vertical farfield profile is 20 degrees. Above 2.2 W instabilities in the L-I curve correlated with beam steering effects occur.

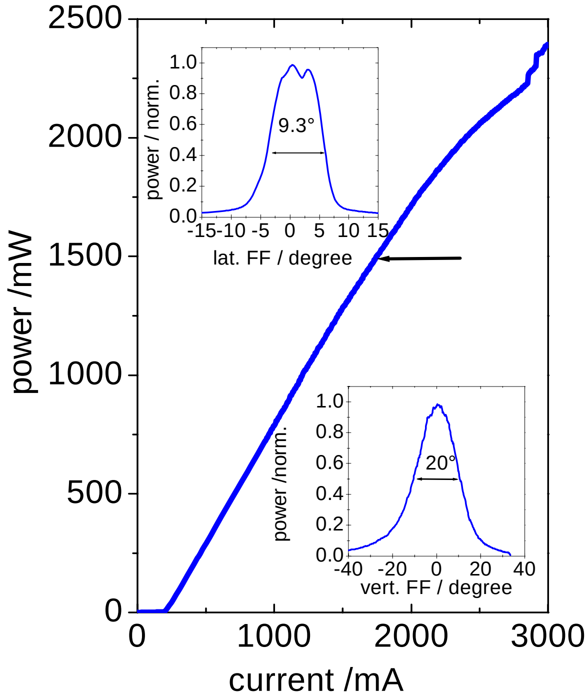

Figure 10. CW light-current characteristic of a 783-nm BA DFB laser at 25°C. Insets: Normalized lateral (top) and vertical (bottom) farfield profiles at an output power of 1.5 W (see arrow).

The variation of the FWHM and the full $1/e^2$ width of the lateral farfield profile with increasing injection current are shown in Fig. 11. With increasing injection current from 0.5A to 2A the farfield broadens from about 6 to 9 degrees (FWHM) respective 9 to 14 degrees ($1/e^2$).

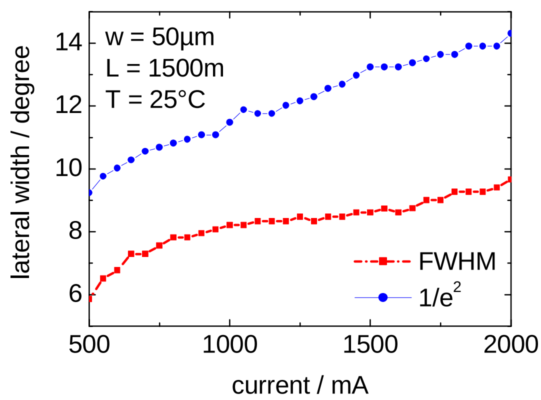

Figure 11. Variation of the FWHM and the full $1/e^2$ width of the lateral farfield profile of the 783-nm BA DFB lasers versus injection current.

The optical spectra of the BA DFB laser (see Fig. 10) measured between 0.5 W and 2 W are depicted in Fig. 12. The spectrum is predominantly single mode up to 0.5 W. Above this power, several peaks are visible and the spectrum broadens. However, the spectral line is still very narrow up to 2 W output power. The full $1/e^2$ width of the spectrum is

0.08 nm at 0.5 W and broadens to 0.20 nm at 1 W. However, a further increase of the power to 2 W slightly reduces the linewidth again to 0.16 nm.

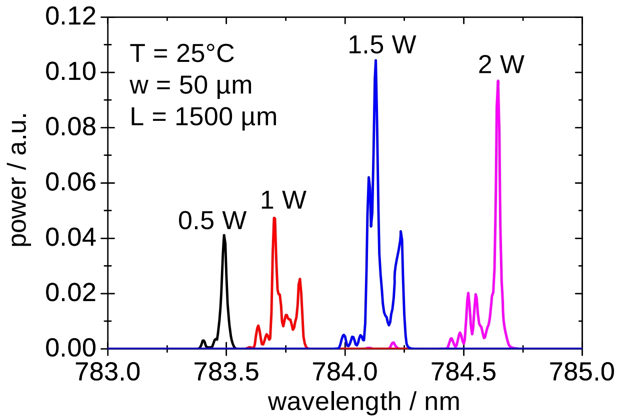

Figure 12. CW optical spectra for the 783-nm BA DFB laser between 0.5 W and 2 W output power at 25°C heatsink temperature.

4. SUMMARY

We have presented experimental investigations on ridge-waveguide (RW) and broad-area (BA) DFB lasers emitting in the wavelength range between 760 and 790 nm. With RW-DFB lasers an output power of more than 300 mW in the TM mode is reached. The optical spectra show single mode emission with a side-mode suppression ratio of more than 50 dB. The measured linewidth of these lasers is 2 MHz. The lateral far field intensity reveals stable lasing of the fundamental mode without any beam steering up to 250 mW, where the lateral far field angle is 12°, and the vertical far field angle is about 21°. By tuning the wavelength with injection current the D_2 line of rubidium vapor was observed. So the performance characteristics of these lasers make them very attractive for atomic spectroscopy. The BA-DFB lasers emit an output power of more than 2 W in a small spectral range of less than 0.20 nm.

ACKNOWLEDGMENTS

The authors thank M. Gielow, R. Olschewsky and J. Hopp for technical support and assistance.

REFERENCES

/1/ S. Stry, R. Knispel, L. Hildebrandt, and J. Sacher, "Compact tuneable diode laser with diffraction limited 500 mW and their application in BEC and CDRS," TDLS, Zermatt, 2003.

/2/ R. D. Martin, S. Forouhar, S. Keo, R. J. Lang, R. G. Hunsperger, R. C. Tiberio and P. F. Chapman, "CW performance of an InGaAs-GaAs-AlGaAs laterally-coupled distributed feedback (LC-DFB) ridge laser diode", IEEE Photon. Techn. Lett., VOL **7**, No.3, 1995, pp 244-246

/3/ J. Wiedemann, K. Ebihara, H.C. Kim, B. Chen, M. Ohta, K. Matsui, S. Tamura, J.-I. Shim, S Arai, "1.5µm wavelength distributed reflector lasers with vertical grating", *Electron. Lett*, VOL **37**, 2001, pp. 831-832,

/4/ L. Hofmann, A. Klehr, A. Knauer, V.B. Smirnitzki, J. Sebastian, and G. Erbert, "120 mW tunable DBR lasers emitting at 1060nm", Electr. Lett. VOL **36**, No.1, 2000, pp 38-39

/5/ H. Wenzel, A. Klehr, M. Braun, F. Bugge, G. Erbert, J. Fricke, A. Knauer, M. Weyers and G. Tränkle, "High-power 783 nm distributed-feedback laser", Electr. Lett. VOL **40**, No. 2, 2004, pp 123-124

/6/ L. Hofmann, A. Klehr, A. Knauer, V.B. Smirnitzki and W. Stolz, "DBR lasers emitting at 1060nm with first-order grating in (InGa)P waveguide layer", Electr. Lett. VOL **35**, No.11, 1999, pp 902-903

/7/ K. Inoguchi, H. Kudo, S. Sugahara, S. Ito, H. Yagi, and H. Takiguchi, “Operation of 780 nm AlGaAs distributed feedback lasers at 100°C with low-loss waveguide structure”, *Jpn. J. Appl. Phys.*, VOL **33**, 1994, pp 852-855

/8/ N.A. Morris, J.C. Conolly, R.U. Martinelli,, J.H. Abeles, and A.L.Cook, “Single-mode distributed-feedback 761-nm GaAs-AlGaAs quantum-well laser”, *IEEE Photon. Techn. Lett.*, VOL **7**, 1995, pp 455-457

/9/ H. Wenzel, M. Braun, J. Fricke, A. Klehr, A. Knauer, P. Ressel, G. Erbert. And G. Tränkle, “High-power ridge-waveguide distributed-feedback lasers emitting at 860 nm”, *Electronics Lett.*, VOL **38**, 2002, pp 1676-1677

/10/ H. Wenzel: “Green’s function based simulation of the optical spectrum of multisection lasers”, *IEEE J. Select. Top. Quant. Electron.* VOL **9**, 865-871, 2003.

/11/ H. Wenzel, A. Klehr, M. Braun, F. Bugge, G. Erbert, J. Fricke, A. Knauer, P. Ressel, B. Sumpf, M. Weyers and G. Tränkle, “Design and realization of high-power DFB lasers,” *Proc. SPIE*, vol. 5594, to be published.

/12/ Th. Kinder, K.-D. Salewski: “Characterizing tuneable external cavity semiconductor lasers using a homodyne fibre interferometer”, *Optik (Jena)* VOL **111**, pp. 127-131, 2000.